Journal of Non-Crystalline Solids 405 (2014) 124–128

Contents lists available at ScienceDirect

Journal of Non-Crystalline Solids

journal homepage: www.elsevier.com/locate/jnoncrysol

Channel diffusion in a lithium–potassium metasilicate glass using the isoconfigurational ensemble: Towards a scenario for the mixed alkali effect

C. Balbuena, M.A. Frechero, R.A. Montani *

Departamento de Química - INQUISUR, Universidad Nacional del Sur, Av. Alem 1253, 8000 Bahía Blanca, Argentina

ARTICLE INFO

Article history:
Received 18 June 2014
Received in revised form 25 August 2014
Accepted 1 September 2014
Available online xxxx

Keywords:
Silicate glasses;
Molecular Dynamics;
Transport channels;
Ionic conductivity;
Mixed alkali effect

ABSTRACT

Performing Molecular Dynamic simulations and using the isoconfigurational ensemble method, we studied the effect of the potassium cation replacing the half part of lithium ions in glassy Li_2SiO_3. This so-constructed glassy system has the main ingredients present in an immediate forthcoming definition of mixed alkali effect (MAE) in glasses. We show the existence of dynamic correlations among the cations of the same species, i.e. Li–Li and K–K, whereas a very weak correlation was observed between a distinct pair of cations. With this novel approach we can put into evidence that the alkali ion diffusion evolves in specific channels for the ions: a Li ion prefers the lithium ion channel and a K ion prefers the potassium ion channel. This result is coincident with previous simulational studies using the bond–valence technique to reverse Monte Carlo and recent experimental findings using quasielastic neutron scattering.

1. Introduction

Relaxation processes in glasses and their inherent manifestations as electrical (ionic) conductivity are still far from being understood at the microscopic scale. Their comprehension plays at present an increasingly urgent role in technology, where considerable progress has been made recently on (for instance): solid-oxide fuel cells, thin film solid electrolytes, electrochemical sensors, supercapacitors, electrochromic windows, etc. For a closer understanding of the ion dynamics in glasses, the study of paradigmatic systems appears as pertinent because (beyond its particular importance) it allows us to extract the essential ingredients of the dynamics, and consequently propose a theoretical scenario for this drama. Silicate glasses are in this direction an appropriate candidate for these purposes in the particular chapter of oxide glasses.

One of the usual concepts inherent to the ion dynamics in oxide glasses, is the concept of “channel” for the diffusion of the moving alkali cations. This concept is closely bounded to the Modified Random Network scenario proposed by Greaves [1] and it proves to be useful to rationalize experimental results. Of course, the concept of channel in glasses is quite different from that employed in crystalline solid electrolytes where the periodic structure plays an essential role in its definition.

The existence of the channels in silicate glasses has been put into evidence theoretically by using the Molecular Dynamics formalism [2], [3], [4], [5], [6], [7], [8] and both theoretically and experimentally in silicate melts [9], [10], [11].

The present authors have shown the existence of these channels in lithium metasilicate glasses in a completely alternative manner to the usual approach [12], [13] by using the isoconfigurational ensemble method (ICEM) proposed by Harrowell et al. [14]. In fact, the use of the ICEM allowed us to put into evidence the existence of similar channels (the same portion of the space) which are found using the pioneering way by Jund et al. [15]. Besides, this methodology has revealed how the local structure and dynamics of the mobile particles in the ‘cage regime’ are the precursors of the dynamics in the diffusive regime [16]. Moreover, it allows us to put into evidence the dynamical connectivity among the ions moving inside the channels [17].

Then the purpose of the present work is to extend our procedure as used on single (lithium) metasilicate glasses to metasilicate mixtures (lithium–potassium). This subject appears pertinent because it defines one of the long standing puzzles of the glass science whose origins are poorly understood: the mixed alkali effect. In a few words, when at a given temperature in a single alkali silicate glass (among many other examples) a systematic substitution by a second alkali oxide occurs, it leads to drops in conductivity of many orders of magnitude before increasing again to the ionic conductivity values corresponding to the second alkali silicate [18]. From different experimental studies [19], [20], [21] it is commonly accepted that the origin of MAE has structural

---

* Corresponding author.
E-mail address: rmontani@criba.edu.ar (R.A. Montani).

http://dx.doi.org/10.1016/j.jnoncrysol.2014.09.001

character. A recent reference to the “state of the art” of the MAE (among other topics of the ion conduction in disordered solids) can be found in the review by Dyre et al. [22].

One attempt to explain this effect is found in the dynamic structure model (DSM) [23], [24] which invokes the mismatch concept: each type of cation generates its own characteristic local environment corresponding to an energy minimum. In this model (and its successive improvements) the relaxation time and the potential energy associated with the ion site depend on the type of ion, each ion creating its own preferred pathway in the network, and participating in the evolution of the energy landscape.

On the other hand, Swenson and Adams, using the Bond Valence analysis of transport pathways to Reverse Monte Carlo method, showed that the two types of alkali ions were randomly mixed and have distinctively different conduction static pathways of low dimensionality [25], [26].

Thus in the present paper we will address the dynamical aspects emerging in a system consisting of a mixture of alkali cations silicate glasses, by comparing them with the two related single alkali glasses. To do that we use the formalism of the Molecular Dynamics (MD) and the ICEM applied to the study of the mixture $(Li_2O)_{0.5}(K_2O)_{0.5}(SiO_2)$.

From the dynamic/structural approach undertaken in this paper, we note that the existence of the dynamic correlation between the mobile ions and the presence of dynamic pathways, allow us to support the scenario proposed in [26] to describe the mixed alkali effect model.

2. Computer simulations

Classical molecular dynamics calculations were performed on a system of 3456 particles (576 Li, 576 K, 576 Si and 1728 O). The system particles interact by the pair potential of Gilbert-Ida type [27] including the r^{-6} term:

$$U_{ij}(r) = \frac{q_i q_j e^2}{4\pi\varepsilon_0 r} - \frac{c_i c_j}{r^6} + f_0\left(b_i + b_j\right)\exp\left(\frac{a_i + a_j - r}{b_i + b_j}\right) \tag{1}$$

The first term in Eq. (1) is the Coulomb interaction with the effective charge numbers q_i, the second term is a dispersive interaction and present for interactions involving only oxygen ions and the last term is a Born–Meyer type potential and takes into account the repulsive short-range interactions.

The parameters of the potentials used were derived on the basis of ab-initio molecular orbital calculations by Habasaki, and the volume of the simulational box ensures that the density corresponds to the experimental density of the glass [28], [29].

The system was prepared by putting the atoms on a cubic box and assigning to each atom velocities drawn from a Maxwell–Boltzmann distribution corresponding to a temperature of 3000 K. The Verlet Algorithm with a time step of 1 fs was used to integrate the equations of motion. Simulations were performed on a cubic box with periodic boundary conditions using the LAMMPS package [30] at two temperatures (700 K and 950 K) well bellow from the calculated Tg which is equal to 1150 K.

The system was equilibrated at 3000 K in a 2 ns run using the NVE ensemble. Then to reach the working temperature, the system was cooled down from 3000 K to its two final temperatures 950 K or 700 K in 2 cooling steps. Each cooling step (from 3000 K to 2000 K, and from 2000 K to 950 K or 700 K) consists of a 2 ns run using a thermostat to decrease the temperature linearly in the NPT ensemble. Two intermediate periods of equilibration consisting of a 2 ns run in the NPT ensemble were included at 2000 K and at 950 K and 700 K to verify no pressure and temperature drifts. After cooling the system, alternate runs of 100 ps each in the NVE and NVT ensemble were successively repeated to complete 2 ns. Then, the system was equilibrated in a 2 ns run using the NVE ensemble. After this equilibration procedure, trajectories of 2 ns length were generated in the NVE ensemble for analysis. We calculate the Tg value from the change in the slope in a volume–temperature curve by performing our simulations in the NPT ensemble. The cooling rate was 4.75 10^{12} K/s.

The usual quantities of interest, such as mean square displacement (MSD): $<r^2(t)>$, the non-Gaussian parameter: $\alpha_2(t)$ were calculated. The mean square displacement $<r^2(t)>$ is defined as:

$$\left\langle r^2(t)\right\rangle = N^{-1}\sum_{j=1}^{N}\left\langle\left|\vec{r}_j(t) - \vec{r}_j(0)\right|^2\right\rangle \tag{2}$$

Where $\vec{r}_j(t)$ is the position vector of particle j at instant t and N is the number of the j-particles. The non-Gaussian parameter $\alpha_2(t)$ is defined as:

$$\alpha_2(t) = \frac{3}{5}\frac{\left\langle r^4(t)\right\rangle}{\left\langle r^2(t)\right\rangle^2} - 1 \tag{3}$$

The non-Gaussian parameter $\alpha_2(t)$ was introduced by Rahman in his pioneering work, and it is a measure of the deviation from the Gaussian form of the van Hove self-correlation function defined in Eq. (5). Then, the time when $\alpha_2(t)$ reaches its maximum value t^* defines a time interval in which the behaviour of the system is dynamically heterogeneous [31]. This quantity is located roughly at the crossover from the caging to the diffusive regime [12].

As mentioned above, we introduced the isoconfigurational ensemble method (ICEM) proposed by Harrowell et al. [14]. In it, one performs a series of equal length MD runs from the same initial configuration; that is, always the same structure but each one with different initial particle momenta chosen at random from the Maxwell–Boltzmann distribution at the appropriate temperature. Then, having been averaged over the initial influence of the momenta, the observed spatial correlations must be configurational in origin. Accordingly, the propensity of a particle for motion in the initial configuration for a fixed time interval t, has been defined as [14]:

$$\left\langle \Delta r_j^2\right\rangle_{IC} = \left\langle\left|\vec{r}_j(t) - \vec{r}_j(0)\right|^2\right\rangle \tag{4}$$

Where $\left|\vec{r}_j(t) - \vec{r}_j(0)\right|^2$ is the squared displacement of particle j (in such time interval) and $< >$ indicates the average over the ensemble (typically 1000 trajectories).

The self space–time correlation function–the van Hove function–$G_s(r,t)$ gives the probability that a particle has moved a distance r in time t. For an isoconfigurational ensemble is written as [32]:

$$G_s(r,t) = {N_{type}}^{-1}{N_{IC}}^{-1}\sum_{j=1}^{N_{IC}}\sum_{i=1}^{N_{type}}\left\langle\delta\left(r - \left|\vec{r}_{ji}(t) - \vec{r}_{ji}(0)\right|\right)\right\rangle \tag{5}$$

Where N_{IC} is the number of trajectories of the ensemble and N_{type} is the total number of i-particles.

3. Results and discussion

3.1. Preliminalia

We have calculated the non-Gaussian parameter $\alpha_2(t)$ for lithium and potassium ions at two temperatures 950 K and 700 K respectively. The non-Gaussian parameter quantifies the deviation of the van Hove function from the Gaussian behaviour. From the results plotted in Fig. 1 we learn that at both temperatures both t^*'s for both kinds of cations are coincident. In the same manner, there is a shift of the peaks to lower times when temperature increases. These similarities strongly

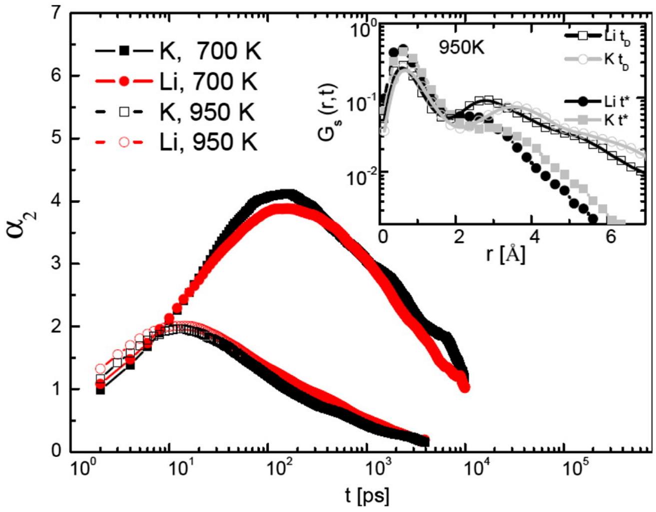

Fig. 1. The non-Gaussian parameter for both kinds of ions at 700 K and 950 K respectively. In the inset: the self-part of the van Hove functions for lithium and potassium ions at two times: t* and t_D (see the text) and at 950 K.

suggest that the same physics are governing the evolution of these two cations.

The inset in Fig. 1, shows the self part of van Hove function at 950 K, for lithium and potassium ions respectively (a qualitatively similar behaviour was observed for 700 K). This function was calculated at two relevant times: $t^* = 20$ ps and $t_D = 130$ ps; the latter value is the time in which the moving ion overcomes the distance across the site of its near neighbours (i.e. it starts a slope with value equal to 1 in a double logarithmic plot of MSD vs. time at 950 K). At 950 K, t* (which roughly corresponds to the end of the caging regime and start of the subdiffusive regime) ions has travelled about 0.7 Å in mean. Following Habasaki and Ngai, this time corresponds to "the primitive ion hopping relaxation time of the coupling model" [33]. In that figure, a shoulder situated approximately at 2.6 Å and at 3.1 Å (for Li and K ions respectively) appears and indicates the existence of an incipient cage decay regime at t*. At t_D, this shoulder develops in a second peak with the concomitant decrease in the area under the first peak, indicating that the number of moving ions (Li or K) that have left from their original sites now becomes significant and takes part in a cooperative regime of motion.

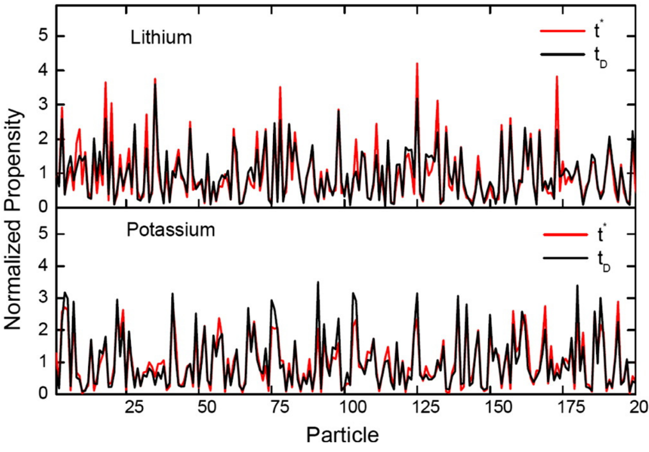

Fig. 2. Normalized propensity of a collection of 200 lithium and potassium ions respectively chosen at random, at 950 K and at two time intervals: t* and t_D respectively (see the text).

3.2. The existence of channels

The ICEM formalism is directly bounded to the notion of propensity to movement of the particles. In our previous work we introduced the high propensity clusters concept (HPC), which defines a topological region of the glassy matrix characterized by its high ability to promote the faster motion of lithium ions: the channels for ionic transport [12].

In Fig. 2 we show the propensity calculated using Eq. (4) for lithium and potassium ions at t* and t_D respectively. Then, from this figure we learn that short and long time behaviours regarding the propensity distribution are similar for the two kinds of alkali cations.

Then, we search for the HPCs following a similar procedure we employed in our previous work [12]. Briefly, the 15% of lithium (or potassium) ions having the higher propensities at time t* are taken as the HPPs (high propensity particles). This fraction at time t* involves those cations having a displacement greater than 2.3 Å, which is roughly the distance of the first minimum in their respective van Hove functions. Following, a three-dimensional array of these HPPs is obtained by plotting a sphere of radius $(\langle \Delta r^2 \rangle_{IC})^{1/2}$, at the initial positions $(t = 0)$ of the HPPs. We found that many of these topological objects are connected among them defining a high propensity cluster: the HPCs. We identify these HPCs to the conduction channels in glasses [17].

One question which arises here is: is the exploration of a narrow time window (defined by t*) enough to define a HPC ("channel") which is supposed to prevail in the diffusive in a nanosecond scale? To answer this question we proceed as in our previous paper [13]: from a 1 ns long MD trajectory at 950 K we select three configurations at three different times: 0, 500 ps and 1000 ps respectively. Then, each one of these three configurations was used as a starting point to construct three isoconfigurational ensembles. At this point it is pertinent to recall that after 500 ps the mobile cations are in their diffusive regime whereas the rest of the glassy matrix remains fixed. At 500 ps the Li and K cations have moved in average distance of 5.2 Å and 6.5 Å respectively, which is well beyond the nearest neighbours.

Then, following the same way described in our previous work [13], in each of these three configurations we search for the HPCs defined by lithium and potassium ions of high propensity (the LiHPs and KHPs). To put into evidence the degree of clusterization or spatial correlation among the LiHPs and among the KHPs we use the following function:

$$f_{HP-\alpha}(r) = \left\langle N_{HP}^{-1} \sum_{i=1}^{N_{HP}} \frac{1}{N_i(r)} \sum_{j=1}^{N_\alpha} \delta\left(r - r_j + r_i\right) \right\rangle \qquad (6)$$

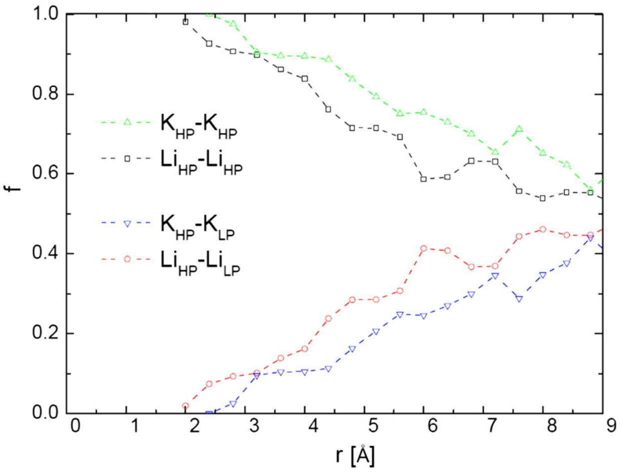

Fig. 3. Fraction of the degree of clusterization or spatial correlation among the LiHPs and among KHPs defined by Eq. (6). (Line is a guide to the eye.)

Eq. (6), gives the fraction of an α-type atom at position r given that a LiHP (or KHP) is at the origin $r = 0$. Here α indicates a high propensity cation (LiHP and KHP respectively) or a low propensity cation (LiLP and KLP respectively). The low propensity cations (LiLP ó KLP) are the same in number as the cations chosen as high propensity ones, but in this case having the lower values of propensities [17].

In Eq. (6), $N_i(r)$ the number of lithium ions placed at the distance r of the reference ion and N_{HP} is the number of high propensity cations (Li or K) involved in the calculation. The brackets indicate the average over the 3 ensembles (0, 500 ps and 1000 ps respectively). Fig. 3 clearly shows the remarkable correlation among the HPs, whereas among the LPs this correlation is lower than the mean value.

3.3. The role of the channels in a scenario for the MAE

Up to this point we just show the existence of conduction channels for lithium and potassium ions, in a similar manner as described in our previous work [12,17,13].

Now, we will address the dynamical correlation among the ions inside these channels. To do that we will use Pearson's correlation coefficient, K_{ij} [34,35]. The value of K_{ij} lies in the [−1,1] interval. It takes the value of 1 in the case of a "complete positive correlation" and on the contrary, it takes the value of −1 for the case of a "complete negative correlation." A value near zero indicates that the involved variables are uncorrelated.

For our particular case, we consider two particles (i, j) of the system separated by a distance r_{ij} and calculate their mean displacement in an isoconfigurational ensemble: $<r_i>_{IC}$ and $<r_j>_{IC}$ respectively, and then compare in each wth-trajectory of the ensemble their displacement in relation to the corresponding mean value. Of course this analysis is performed at a given time; in our case, the relevant t*. Then, for two particles i, j separated at a given distance r_{ij}, in the ensemble, the analytical expression of K_{ij} takes the following form:

$$K_{ij}\left(r_{ij}\right) = \frac{\sum_{w=1}^{N_{IC}} \left(\langle r_i\rangle_{IC} - r_i(w)\right) \cdot \left(\langle r_j\rangle_{IC} - r_j(w)\right)}{S_i \cdot S_j} \tag{7}$$

Where N_{IC} is the total number of trajectories in the isoconfigurational ensemble and S_i and S_j are the standard deviation of the displacement in the calculated trajectory of the ensemble.

We calculate using Eq. (7) and plot in Figs. 4 and 5, the Pearson's correlation coefficient for the Li–Li and Li–K pairs which are diffusing in a "lithium channel": HPC_{Li}–Li and HPC_{Li}–K respectively. Similarly, for the K–K and K–Li pairs moving into "potassium channel": HPC_K–K and HPC_K–Li. In these figures and the respective partial pair, distribution functions are included.

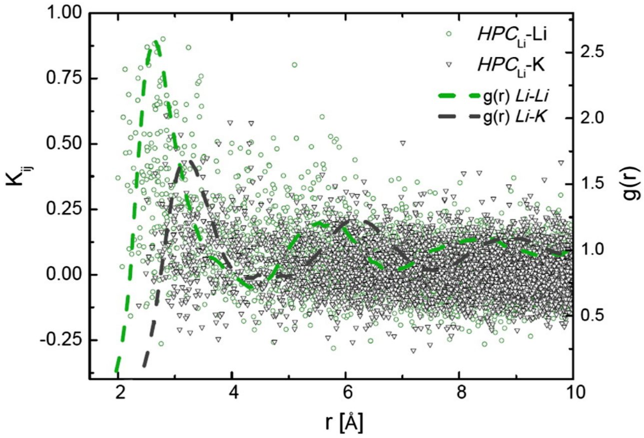

Fig. 4. The radial distribution function for lithium–lithium and lithium–potassium, and $K_{Li–Li}$ and $K_{Li–K}$ in a lithium channel, at 700 K.

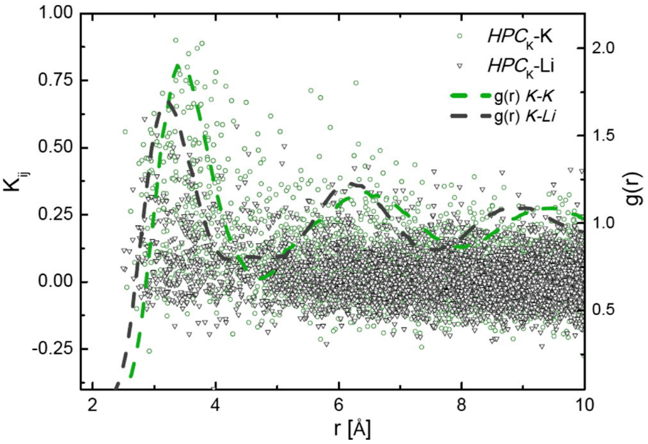

Fig. 5. The radial distribution function for potassium–potassium and potassium–lithium, and $K_{K–K}$ and $K_{K–Li}$ in a potassium channel, at 700 K.

In Fig. 4 it becomes clear for the lithium channel that (for example) over the value 0.2–which ensures an acceptable degree of correlation–the values of $K_{Li–Li}$ are strongly concentrated under the first peak of its corresponding $g_{(r)}$. Conversely, the $K_{Li–K}$ values indicate a poor or non-existent correlation. A completely equivalent explanation holds for the potassium channel in Fig. 5: the values of of $K_{K–K}$ are strongly concentrated under the first peak of its corresponding $g_{(r)}$. Conversely, the $K_{K–Li}$ values remain under 0.2 indicating a poor or nonexistent correlation.

Then a high value of K_{ij} between two ions of the same species indicates that in this portion of the sample these ions are dynamically connected (its dynamics is facilitated). Then from Figs. 4 and 5 we can conclude that these topological regions of the sample are *specific* for the diffusion of the same kind of ions: in other words, there are exclusively channels for lithium ions and for potassium ions respectively.

The previous results are clearly and qualitatively summarised and shown in Fig. 6. In this figure, we plot the distribution of K_{ij} between neighbours at a distance lower than 4.5 Å corresponding to the first minima in the partial pair distribution functions for the Li–Li, Li–K and K–K pairs respectively. Clearly for the unlike pairs the probability is strongly concentrated at a value equal to 0.1 for K, whereas for the pairs of the same kind of ions the distribution is displaced to the higher values of K.

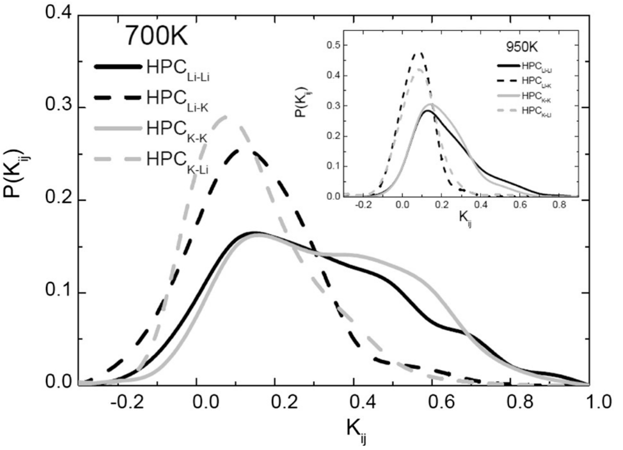

Fig. 6. The distribution of K_{ij} at 700 K and 950 K (shown in the inset) on the length scale of the nearest-neighbour distance (first minima in the partial pair distribution functions for the Li–Li, Li–K and K–K pairs respectively).

This figure also attends to a very important experimental fact present the MAE in its connection with temperature. Effectively, the specificity of the channels is stronger at the lower temperature and could contribute to condition (hinder) the ionic transport. On the other hand, the preferred pathways (specificity) effect disappears at higher temperatures probably mainly due to thermal effects.

4. Conclusion

In this paper we report our studies on the alkali cation dynamics in glassy $LiKSiO_3$. We use the Molecular Dynamics formalism and the isoconfigurational ensemble method. The isoconfigurational ensemble method and Pearson's coefficient allowed us to calculate the correlation among the displacements of the moving cations. Our results confirm the existence of dynamic correlations among the cations of the same species, i.e. Li–Li and K–K, whereas a very weak correlation was observed between an unlike pair of cations. That is, our results clearly indicate that the alkali ion diffusion in silicate evolves in specific channels for the ions: a Li ion prefers the lithium ion channel and a K ion prefers the potassium ion channel; channels whose existence is underlying in the short time dynamics, even in the caging regime. The existence of preferred (specific) pathways for conduction on silicate melts was recently put into evidence experimentally by Meyer et al. [10], [11] from a structural point of view, using quasielastic neutron scattering. On the other hand Swenson and Adams showed using the bond-valence technique to reverse Monte Carlo–i.e. a structural study–that two types of alkali ions in a mixed alkali glass have distinctly different conduction pathways meaning that *A* ions block the pathways for the *B* ions and vice-versa. These authors concluded that this blocking effect is the main reason for the experimentally observed MAE [36]. Moreover, Habasaki and co-workers have emphasized–from a dynamical point of view–the importance of the cooperative blockage as the mechanism responsible for the MAE [36]. Thus, we conclude here saying that due to the intrinsic nature of our study it confirms in a more comprehensive (general) manner these previous findings.

Acknowledgement

Financial support from UNS, ANPCyT, SeCyT and CONICET is gratefully acknowledged. R.A.M. is a research fellow of the C.I.C. and M.A.F. is a research fellow of CONICET. C.B. thanks CONICET for a fellowship.

References

[1] G.N. Greaves, K.L. Ngai, Phys. Rev. B52 (1995) 6358.
[2] J. Horbach, W. Kob, K. Binder, Phys. Rev. Lett. 88 (2002) 125502.
[3] C.H. Lammert, A. Heuer, Phys. Rev. B70 (2004) 24204.
[4] E. Müller, S. Zienicke, J. Adams, Habasaki, P. Maass, Phys. Rev. B75 (2007) 14203.
[5] P. Rao, T.D. Tho, S. Adams, Solid State Ionics 181 (2010) 1.
[6] Stefan Adams, R. Prasada Rao, Phys. Chem. Chem. Phys. 11 (2009) 3210.
[7] S. Balasubramanian, K.J. Rao, J. Non-Cryst. Solids 181 (1995) 157.
[8] J. Habasaki, I. Okada, Y. Hiwatari, J. Non-Cryst. Solids 183 (1995) 12 (208, 181 (1996)).
[9] F. Kargl, A. Meyer, M.M. Koza, H. Schober, Phys. Rev. B74 (2006) 14304.
[10] K. Binder, J. Horbach, H. Knoth, P. Pfleiderer, J. Phys. Condens. Matter 19 (2007) 205102.
[11] A. Meyer, F. Kargl, J. Horbach, Neutron News 23 (2012) 35.
[12] R.A. Montani, C. Balbuena, M.A. Frechero, Solid State Ionics 209–210 (2012) 5.
[13] C. Balbuena, M.A. Frechero, R.A. Montani, Solid State Ionics 255 (2014) 135.
[14] A. Widmer-Cooper, P. Harrowell, H. Fynewever, Phys. Rev. Lett. 93 (2004) 135701.
[15] P. Jund, W. Kob, R. Jullien, Phys. Rev. B 64 (2001) 134303.
[16] A. Widmer-Cooper, P. Harrowell, Phys. Rev. Lett. 96 (2006) 185701.
[17] C. Balbuena, M.A. Frechero, R.A. Montani, J. Non-Cryst. Solids 369 (2013) 17.
[18] M.D. Ingram, Phys. Chem. Glas. 28 (1987) 215.
[19] J. Swenson, A. Matic, C. Karlsson, L. Borjesson, C. Meneghini, W.S. Howells, Phys. Rev. B 63 (2001) 132202.
[20] S.N. Houde-Walter, J.M. Inman, A.J. Dent, G.N. Greaves, J. Phys. Chem. 97 (1993) 9330.
[21] A.T.W. Yap, H. Förster, S.R. Elliott, Phys. Rev. Lett. 75 (1995) 3946.
[22] J.C. Dyre, P. Maass, B. Roling, D. Sidebottom, Rep. Prog. Phys. 72 (2009) 46501.
[23] P. Maass, A. Bunde, M.D. Ingram, Phys. Rev. Lett. 68 (1992) 3064.
[24] A. Bunde, M.D. Ingram, S. Russ, Phys. Chem. Chem. Phys. 6 (2004) 3663.
[25] S. Adams, J. Swenson, Phys. Chem. Chem. Phys. 4 (2002) 317.
[26] J. Swenson, S. Adams, Phys. Rev. Lett. 90 (2003) 155507.
[27] Y. Ida, Phys. Earth Planet. Inter. 13 (1976) 97.
[28] J. Habasaki, I. Okada, Mol. Simul. 9 (1992) 319.
[29] R.D. Banhatti, A. Heuer, Phys. Chem. Chem. Phys. 3 (2001) 5104.
[30] S.J. Plimpton, J. Comp. Physiol. 117 (1995) 1.
[31] A. Rahman, Phys. Rev. 136 (1964) A405.
[32] J.P. Hansen, I.R. McDonald, Theory of Simple Liquids, 2nd. Ed Academic Press, London, 1986.
[33] J. Habasaki, K. Ngai, Phys. Chem. Chem. Phys. 9 (2007) 4673.
[34] A. Widmer-Cooper, P. Harrowell, J. Chem. Phys. 126 (2007) 154503.
[35] W.H. Press, B.P. Flannery, S.A. Teukolsky, W.T. Vetterling, Numerical Recipes. The art of Scientific Computing, Cambridge University Press, 1986.
[36] J. Habasaki, K. Ngai, Y. Hiwatari, J. Chem. Phys. 121 (2) (2004) 925.